CAVITY DIAGNOSTICS USING ROTATING MAPPING SYSTEM FOR 1.3GHz ERL 9-CELL SUPERCONDUCTING CAVITY

Hiroshi Sakai#, Takaaki Furuya, Takeshi Takahashi, Shogo Sakanaka, Kensei Umemori,
KEK, Tsukuba, Ibaraki, 305-0801, Japan
Kenji Shinoe, ISSP, University of Tokyo, Kashiwa, Chiba, 277-8581, Japan
Masaru Sawamura, JAEA, Tokai, Naka, Ibaraki, 319-1195, Japan

Abstract

We are developing the superconducting (SC) cavity for Energy Recovery Linac (ERL) in Japan[1]. In order to survey the electron emission and the heating spot of the cavity inner surface in detail, cavity diagnostics with the rotating mapping system was applied. Two types of sensors, one of which was the carbon resistor and the other was the Si PIN photo diode, were set to detect the temperature rise and electron emission. By rotating the sensor arrays around the cavity axis, a lot of information was obtained all over the cavity surface in detail. This paper reports the results of vertical tests by using this rotating mapping system with the Nb 9-cell ERL cavity.

INTRODUCTION

The development of the superconducting cavity is one of the most important issues to realize high current energy recovery linacs (ERLs). Most challenging task is a strong damping of higher-order-modes (HOMs) to avoid beam-breakup instabilities and to suppress heat loads on cryomodules. Figure 1 shows a conceptual design of our cavity named as "KEK-ERL model-2 cavity". Salient features of this cavity compared with the TESLA-type cavity are as follows. The first is adopting the enlarged beam pipes, whose diameters is 100mm (Small Beam Pipe (SBP)) & 120mm (Large Beam Pipe (LBP)) to extract HOMs from cavity. The second is applying the Eccentric-fluted beampipe (EFB) to suppress quadrupole HOMs[2]; the third is changing the cell shape and iris diameter to 80mm to reduce the R/Q's of HOMs. The strategy of designing of this cavity is expressed in Ref.[3]. This design satisfies more than 100mA current ERL operation. The important task for ERL operation is to clarify that the newly designed cell-shape, enlarged beam pipes and EFB do not enhance the thermal breakdown (TB) and field emission (FE) in a Nb cavity. Sophisticated cavity diagnostics is needed for surveying these sources.

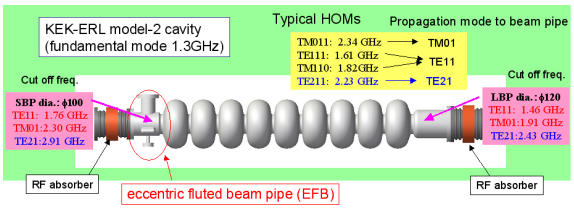

Figure.1: Schematic view of KEK-ERL model-2.

#sakai.hiroshi@kek.jp

The main procedure for studying TB and FE is to measure the heat spot and X-ray radiation on the cavity surfaces at RF operation. We have two choices for measuring temperature and X-ray mapping for 9cell cavity; one is fixed mapping and the other is rotating mapping. The approaches of the fixed mapping were done for single-cell cavity by setting about 700 sensors on cavity surface [4,5]. However, for 9-cell cavity we need more than 6000 sensors for getting the precise mapping and a lot of channels for data taking. On the other hands, the rotating mapping system needs at most 100 sensors and can measure the precise mapping because the angle resolution is determined by the gear and stepping motor resolution. At the TESLA 9-cell cavity, T-mapping was successfully measured by using rotating mapping system [6]. Therefore, we selected the rotating mapping system for the ERL 9-cell cavity. However, in our cavity case, main issue is that the ratio of the surface electric field, Epeak, to the accelerating field, Eacc, (Epeak/Eacc) is 1.5 times higher than that of the TESLA cavity. Especially, iris of this cavity has the largest Epeak. It is important to know the radiation source and to measure the radiation trace precisely to study the FE on the cavity surface including iris part. Therefore, we newly apply the rotating mapping system for getting precise T&X-mapping. To check the performance of new rotating mapping system, we have first applied the rotating mapping system to the Nb single-cell cavity with the same cell shape of KEK-ERL model-2 cavity and have done the vertical tests [7]. The precise T&X-mapping was successfully measured [8]. By using this mapping system, we have found that EFB and large beam pipes do not become the source of electron emission and heating spot. From these results we proceed to fabricate the KEK-ERL model-2 cavity.

SETUP

Figure 2 shows the set-up of the vertical test of KEK-ERL model-2 cavity with the rotating mapping system. Two types of sensor, one of which was the carbon resistor (Allen-Bradrey, 50Ω) and the other was the Si PIN photo diode (HAMAMATSU, S5821-02), were set to detect the heat spot and the X-ray radiation distribution due to emitted electron, respectively. The eight Si PIN diodes per cell and, in addition, one PIN diode per iris were arranged along the cavity as shown in Fig. 3. Totally, 82 PIN diodes were set at the same rotating angle. Unfortunately, the only 36 carbon resistors were set around the cavity because of the lack of logger channel. Each four carbon resistors per cell were set on the equator points at every

90 degrees in Fig. 3. All carbon resistors were embedded in the stycast base so that it worked as a heat sink and pushed by the "pantograph-type" plate springs in order to obtain the sufficient contact between carbon resistors and Nb cavity surface. All PIN diodes and carbon resistors are fixed to the supports. We divided the supports into three parts at every three cells to reduce the force coming from the friction between the carbon resister and cavity and the effect of the pre-tuning error and kink of cavity itself. Each support with sensor arrays was equipped on each gear and turned around the cavity axis by rotating a gear via motor. The three rotation angles of the sensors were controlled by the motor control system individually. Each resistor was provided with 0.1 mA for taking the data of the change of resistance. The generated current at the PIN diode was converted to voltage and amplified 10 times at operational amplifier. These data including sensors, power meters and rotating angle were taken by the real-time data acquisition system (YOKOGAWA, MX-100 & MW-100). Data were taken every 0.5 sec to reduce the AC noise coming from the amplifiers of diodes. All resistors were calibrated with Si diode thermo-sensor under cooling from room temperature to 2K.

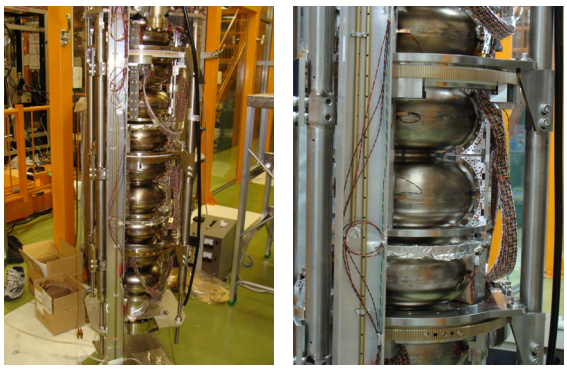

Figure 2: Setup of vertical test with rotating mapping system of KEK-ERL model-2 9cell cavity.

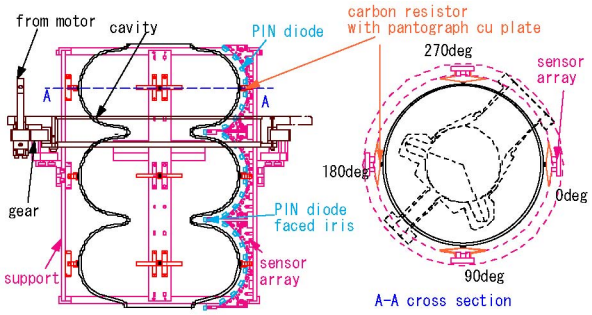

Figure 3: (Left) Detailed setup of mapping system of one support with a gear. Eight PIN diodes (light blue) are set on one cell and one PIN diode faces the iris of cavity. (Right) Cross section of the equator. The carbon resistors (orange) are set around the cavity at every 90 degrees. 0deg shows the initial point of rotating mapping system.

RESULTS OF VERTICAL TESTS

We carried out the eight vertical tests of KEK-ERL model-2 cavity. The rotating mapping system was applied from the 4th vertical test. The 6th and 8th vertical tests were not carried out by the vacuum leak. Then we show the results of T&X mapping of the 4th, 5th and 7th vertical tests. Detailed history of fabrication procedure, the parameters of the surface treatments and vertical tests are expressed in Ref.[9]. During previous three vertical tests, we suffered from many temperature rise and field emission. Before the 4th vertical test, we refresh the inner cavity surface by the additional Electro-polishing with 50μm thickness. We applied no additional surface treatment between the 4th and 5th vertical tests in order to check the reproducibility of Q-E plot and the radiation distribution of cavity.

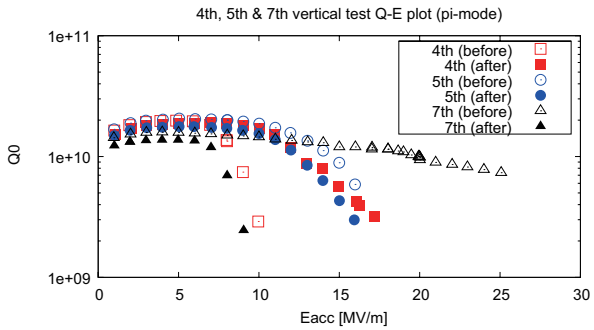

Figure 4: Q-E plot of the 4th , 5th & 7th vertical tests.

Figure 4 shows the Q-E plots of π-mode at 4th, 5th & 7th vertical tests. Each plot shows the results before and after pass-band measurement of vertical tests. We successfully tested the 9cell cavity up to a field gradient of 15 MV/m at 2K. However, we also observed that the Q-value decreased due to field emissions above the field gradient of 10 MV/m at the 4th vertical test. In order to investigate the cause of this problem in detail, we applied the rotating mapping system.

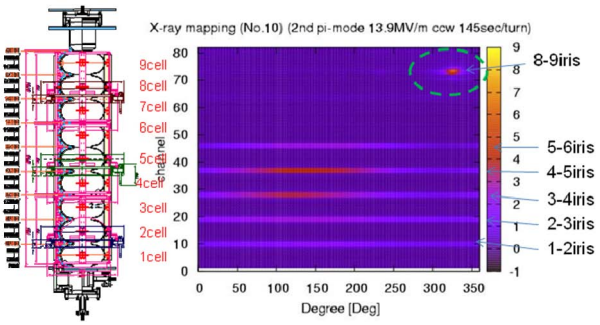

Figure 5: X-mapping result of the 4th vertical test.

Figure 5 shows the results of X-ray radiation mapping at the 4th vertical measurement at 13.9MV/m accelerating field. We have clear strong radiation peak on 8-9 iris nearby of the 330° with 10° FWHM and the broad radiation trace on 1-6 irises in Fig. 5. We detected the large radiation by PIN diode set on the top and bottom

flanges. Finally these radiation peaks did not disappear on the 4th vertical test. In order to survey the emission source again, we done the 5th vertical test. Q-E plot is almost same as the 4th measurement. And we also observed the clear strong peak on 8-9 iris nearby of the 330° with 10° FWHM. The radiation distribution was reproduced at the 5th vertical test. We note that same radiation peak on 8-9 iris nearby of the 330° were also observed when we excited the 8/9π, 7/9π and 6/9π -modes which fields are strong at 8-9 iris. In these three pass-bands, no broad radiation was observed at 1-6 irises. This indicates that radiation sources will be located on 8-9 iris.

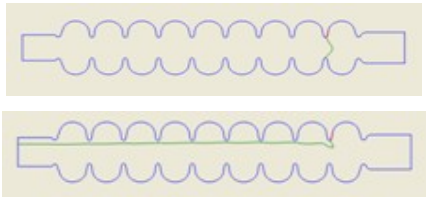

Figure 6: Calculation of electron trace from emission source at 8-9 iris with applying accelerating field. Green line shows the electron trajectory coming from iris.

After the 4th and 5th vertical test, we investigated the inner surface by using the optical inspection camera [10]. We found the large tip on 8-9 iris around 150°, which is just opposite side of 330° of the strong radiation point of green dotted circle of Fig. 5 [9]. By calculation of electron trajectory, we found the emission source would make the radiation peak at opposite side and also make the radiation peak at other iris point as shown in Fig. 6. From these results, we regarded the tip of the iris point as one of the radiation sources. We grinded this tip for recovering the accelerating field from the field emission after the 5th vertical test.

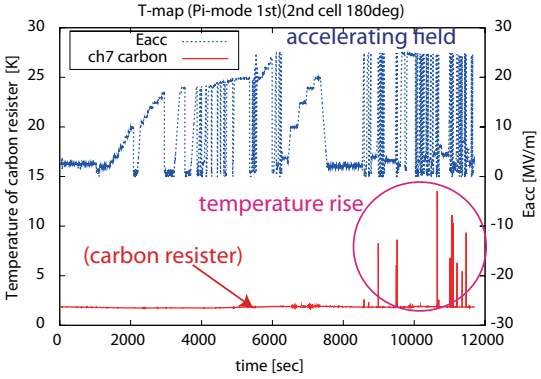

Figure 7: Observation of temperature rises of the 2nd cell 180deg point at 25MV/m accelerating field.

We refreshed the cavity surface by EP and carried out vertical test. The result of Q-E plot of the 7th vertical test was shown in Fig. 5 of triangles. First, accelerating field reached up to 25MV/m. In this case, no other radiation was observed at 18MV/m. By grinding the tip of iris, accelerating field was much improved. Field was limited by the TB. The local heating was observed at the equator of the 2nd cell between 180° and 240° by rotating the carbon resistors as shown in Fig. 7 when the quench occurred at 25MV/m. Unfortunately, when we operated the 6/9π-mode, the sudden radiation burst occurred and resulted in increasing the radiation. Fig. 8 shows the X-ray mapping data of π-mode of the 7th vertical test at 9MV/m accelerating field after pass-band mode measurement. Many radiation peaks were observed. The accelerating field was limited by field emission as shown in Fig. 5 of black solid triangles and did not recover at last.

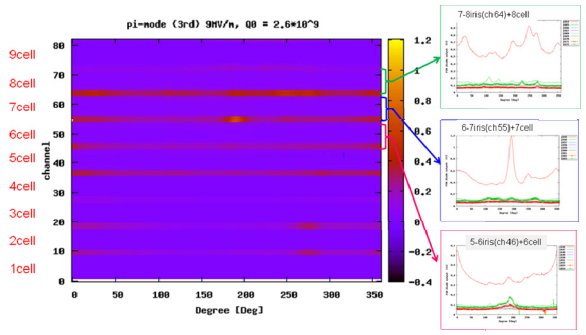

Figure 8: X-mapping result of π-mode of the 7th vertical test at 9MV/m after pass-band mode measurement.

SUMMARY

We have applied the rotating mapping system for the KEK-ERL model-2 9cell cavity. The rotating mapping system worked well at 2K condition. At the 4th and 5th vertical test, we had clear strong radiation peak on 8-9 iris nearby of the 330°. When we investigate the inner surface of cavity, we found the large tip on 8-9 iris around 150°, which was opposite side of strong radiation peak. By grinding this large tip, accelerating field was much improved up to 25MV/m. The rotating mapping system will be a strong tool for surveying the radiation sources and heat spots in details. We now increased the six carbon resistors per cell and to survey the radiation sources in detail by studying the correlation between heat spots and radiation trace with both measurement and calculation.

REFERENCES

[1] T. Kasuga et al., Proc. of PAC07, p1016.
[2] M. Sawamura et al., Proc. of PAC'07, p1022.
[3] K. Umemori et al., Proc. of APAC2007, p. 570.
[4] J. Knobloch et al. Rev. Sci. Instrum., 65:3521 (1995)
[5] R. Roth et. al., Proc. of 5th SRF workshop, p599 (1991)
[6] Q. S. Shu et al, Proc. of PAC95, p1639.
[7] K. Umemori et al., Proc. of EPAC2008, p.925.
[8] H. Sakai et al., Proc. of EPAC2008, p907.
[9] K. Umemori et al. in these proceedings, WEPEC030.
[10] Y. Iwashita et al., Phys. Rev. ST Accel. Beams 11, 093501 (2008).